CHINESE JOURNAL OF PHYSICS VOL. 52, NO. 2 April 2014

A Theoretical Investigation on the Electrical Transport Properties of a Two Dimensional Electron Gas in AlGaN/GaN Heterostructure

Mohammad Amirabbasi*

University of Shahrood, Shahrood, Semnan Province, Iran
(Received May 6, 2013; Revised August 19, 2013)

In this paper I have tried to theoretically investigate the electrical transport properties of the two dimensional electron gas of an $Al_{0.3}Ga_{0.7}N/GaN$ heterostructure, and the most important effective parameters in the temperature-dependent behavior of the carrier mobility in the temperature range of 75 to 350 K have been studied. My analysis indicates that extrinsic scattering mechanisms, such as the ionized impurity due to interface charges and the crystal defects, have an important role in controlling the carrier mobility in this system. Also, in order to obtain good fit at high temperature, I have to change the value of the electron effective mass in this system. With this change, the polar optical scattering mechanism is dominant at high temperature.

DOI: 10.6122/CJP.52.872 PACS numbers: 73.61.Ga

I. INTRODUCTION

GaN is a compound semiconductor of group III -V with a wide direct band gap (3.5 eV) [1] which has been used in manufacturing electronic and optoelectronic devices, such as blue and UV light-emitting diodes [2], blue laser diodes [3], and high temperature field effect transistors [4–6]. Transport properties such as the carrier mobility (μ) are crucially important because the operation of all these devices depend critically on current transport. Alloying GaN with Al and forming an AlGaN/GaN heterostructure with a two dimensional electron gas (2DEG) has been studied recently because of its application in manufacturing heterostructure field-effect transistors (HFETs) and high electron mobility transistors (HEMTs).

In this paper I have tried to theoretically analyze the electrical transport properties of the 2DEG for $Al_{0.3}Ga_{0.7}N/GaN$ heterostructure, which was reported by Polyakov *et al.* [7]. The a-plane GaN sample was grown on an r-plane sapphire substrate using metal–organic chemical vapor deposition (MOCVD). For a heterojunction AlGaN/GaN structure, a 3-nm-thick AlGaN film with Si doping of 3×10^{19} cm^{-3} and a 3-nm-thick undoped GaN cap layer was grown on top of the a-GaN film [7]. The Al mole fraction in the AlGaN barrier was $x = 0.3$ [7]. The sheet carrier concentration of the 2DEG in the system has been reported as around 1.2×10^{13} cm^{-2} [7]. More experimental details have been mentioned in Ref. [7].

*Electronic address: mohammad.ab.98@gmail.com

II. THEORY OF SCATTERING MECHANISMS

Here, the mobility limit due to each individual scattering process is calculated independently, using their corresponding analytical expressions (μ_i). The material parameters used in the calculations are listed in Table I. The details of the scattering mechanism formulas can be seen in Ref. [13]. I have just listed the scattering mechanism formulas in Tables II and III, where L ($= 2(\frac{n_s}{10^{12}\mathrm{cm}^{-2}})^{-1/3} \times 55$ Å) is the width of the quantum well, n_s is the 2DEG sheet carrier density, h_{14} is the piezoelectric constant, k_f ($= (2\pi n_s)1/2$) is the wave vector on the Fermi surface, and

$$I_A(\gamma_t) = \left[\left(\frac{4\gamma_t}{3\pi}\right)^2 + 1\right]^{1/2}, \tag{1}$$

$$I_A(\gamma_l) = \left[\left(\frac{4\gamma_l}{3\pi}\right)^2 + 1\right]^{1/2}, \tag{2}$$

where

$$\gamma_t = \frac{2\hbar u_t k_f}{k_B T}, \tag{3}$$

$$\gamma_l = \frac{2\hbar u_l k_f}{k_B T}, \tag{4}$$

$$1/\varepsilon_p = 1/\varepsilon_\infty - 1/\varepsilon_s. \tag{5}$$

Also $S_0(= \frac{e^2 m^*}{2\pi\varepsilon_0\varepsilon_s\hbar^2})$, the screening constant, is a function of the 2DEG sheet carrier density (n_s) and the lattice temperature (T_L), d_0 is the width of the spacer layer and d_l is the width of the depletion layer ($\approx n_s/N_d$, with N_d as the donor density in the barrier), N_{bi} is the 2D impurity density in the potential well due to background impurities and/or interface charge, N_{disl} is the charge dislocation density, c is the lattice constant of $Al_xGa_{1-x}N$ [$= xa_l(\mathrm{AlN}) + (1-x)a_0(\mathrm{GaN})$ suggested by Vegard's law], ξ is a dimensional parameter: $\xi = 2kF/qT_F$; $qT_F = 2/a_B$ is the 2D Thomas-Fermi wave vector, where $a_B = \varepsilon_s\varepsilon_0 h^2/\pi e^2 m^*$ is the effective Bohr radius in the material and

$$L_0 = d_0 + L/2, \tag{6}$$

$$LM_0 = L_0 + d_1, \tag{7}$$

$$I_B = \int_0^\pi \frac{\sin(\phi)}{\left[2\sin(\phi) + \frac{S_0}{k_f}\right]^2} d\phi, \tag{8}$$

$$I_t = 1/2\xi^2 \int_0^1 \frac{1}{(1+\xi^2 u^2)\sqrt{1-u^2}} d\phi. \tag{9}$$

TABLE I: Values of the GaN material parameters used in the scattering formulas.

material parameters	values
Density of the crystal (ρ) [8]	6.1×10^3 (kg/m^3)
Deformation potential energy (E$_l$) [9]	9.2 (eV)
High-frequency dielectric constant (ε_∞) [10]	$5.47\varepsilon_0$ (Fm^{-1})
Static dielectric constant (ε_s) [10]	$10.4\varepsilon_0$ (Fm^{-1})
Effective mass (m^*) [11]	$0.22m_0$ (kg)
GaN lattice constant (a_0) [12]	0.5185 (nm)
AlN lattice constant (a_l) [12]	0.4982 (nm)

TABLE II: Intrinsic scattering mechanisms formulas.

Acoustic deformation potential scattering	$\mu_{ac}(T) = \frac{e\hbar^3\rho u_l^2 L}{m^{*2}E_l^2 k_B T}$
Piezoelectric scattering	$\mu_{pz}(T) = \frac{\pi k_f E_l^2}{Le^2h_{14}^2}\left[\frac{9}{32} + \frac{13}{32}(\frac{u_l}{u_t})^2\frac{I_A(\gamma_t)}{I_A(\gamma_l)}\right]^{-1}\mu_{dp}$
Polar – optical phonon (LO) scattering	$\mu_{pop}(T) = \frac{4\pi\varepsilon_0\varepsilon_p\hbar^2}{e\omega(m^*)^2 L}\left[\exp(\hbar\omega/k_BT) - 1\right]$

II-1. Calculation of transverse and longitudinal acoustic phonon velocities

The acoustic wave in GaN consists of two longitudinal and transverse components with the velocity u_l and u_t, respectively, which can be obtained from the following relations [14]:

$$u_l = \sqrt{C_{33}/\rho}, \tag{10}$$

$$u_t = \sqrt{C_{44}/\rho}, \tag{11}$$

where C_{33} and C_{44} are the elastic stiffness coefficients, which have been reported as of 395 GPa and 241 GPa, respectively [15].

TABLE III: Extrinsic scattering mechanisms formulas

Ionized impurity scattering due to remote donors	$\mu_{remote}(T) = \frac{64\pi\hbar^3 k_f^3\varepsilon_0^2\varepsilon_s^2 s_0^2}{e^3(m^*)^2 N_d}\left(\frac{1}{L_0^2} - \frac{1}{LM_0^2}\right)^{-1}$
Ionized impurity scattering due to interface charges	$\mu_{bi} = \frac{4\pi\varepsilon_0^2\varepsilon_s^2\hbar^3 k_f^3}{e^3(m^*)^2 N_{bi} I_B}$
Dislocation scattering	$\mu_{disl} = \frac{4\pi\varepsilon_0^2\varepsilon_s^2\hbar^3 k_f^4 c^2}{e^3(m^*)^2 N_{disl} I_t}$

III. RESULT AND DISCUSSION

III-1. Band gap

With respect to Vegard's law and the value of the band gap of GaN (= 3.5 eV) [1] and AlN (= 6.28 eV) [16], I can calculate the value of the $Al_{0.3}Ga_{0.7}N$/GaN band gap about 4.33 eV, that means the $Al_{0.3}Ga_{0.7}N$/GaN band gap is wider than the GaN layer. So it should be expected that part of the conduction electrons in the AlGaN layer are transferred to the adjacent layer with a smaller band gap (GaN), which caused an internal field and, subsequently, the formation of a triangular quantum well, and thus the formation a thin layer near the interface with a 2DEG behavior.

III-2. temperature-dependent carrier mobility

Fig. 1 shows the total mobility of the pure AlGaN/GaN obtained from Matthiesen's rule by considering the intrinsic scattering mechanisms. As seen in Fig. 1, in the pure AlGaN/GaN system, the total mobility at room temperature is on the order of 10^3 (cm^2/Vs). With respect to the experimental data (See Fig. 2), this value decreases (on the order of 10^2 (cm^2/Vs) which is attributed to effects of the extrinsic scattering mechanisms.

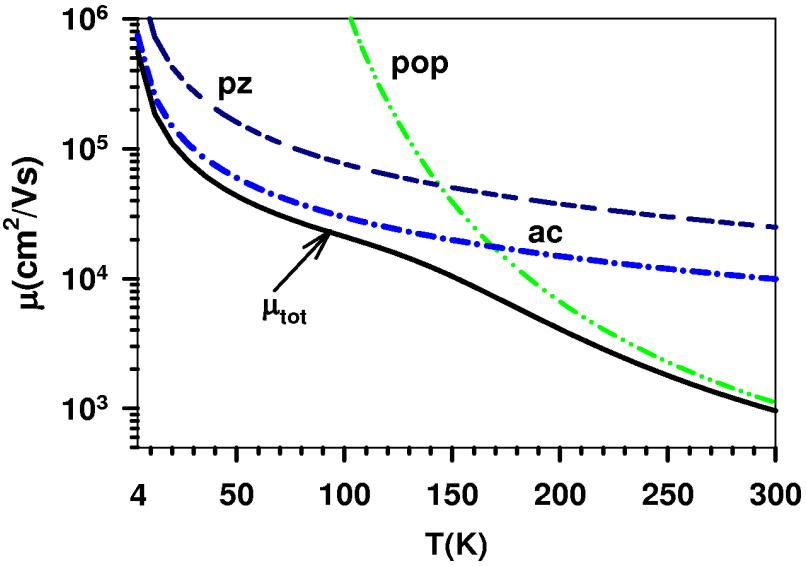

FIG. 1: the total mobility (black solid curve) of hypothetically pure AlGaN/GaN calculated using Matthiesen's rule. The mobility limits due to the lattice scattering events are displayed in the dashed curves.

Fig. 2 shows the experimental data of the temperature-dependent electron mobility in this system from 75 to 350 K. As is clear, in contrast to the GaN bulk layers [17] the electron mobility with decreasing temperature in this condition is first increased and then remains almost constant, which is the result of the 2DEG properties and the elimination of the carrier freeze-out process at low temperature. To analyze these data I have used different

scattering mechanisms, as mentioned in Tables II and III and the material parameters of GaN in Table I. It should be mentioned that during the analysis process the value of the velocities of u_l and u_t, in Equations (10) and (11) have been replaced by 8.04×10^3 (m/s) and 6.28×10^3 (m/s), respectively. Fig. 1 shows the related position for each of the scattering mechanisms, and Tables IV and V show the value of the fitting parameters which have been used in this theoretical analysis.

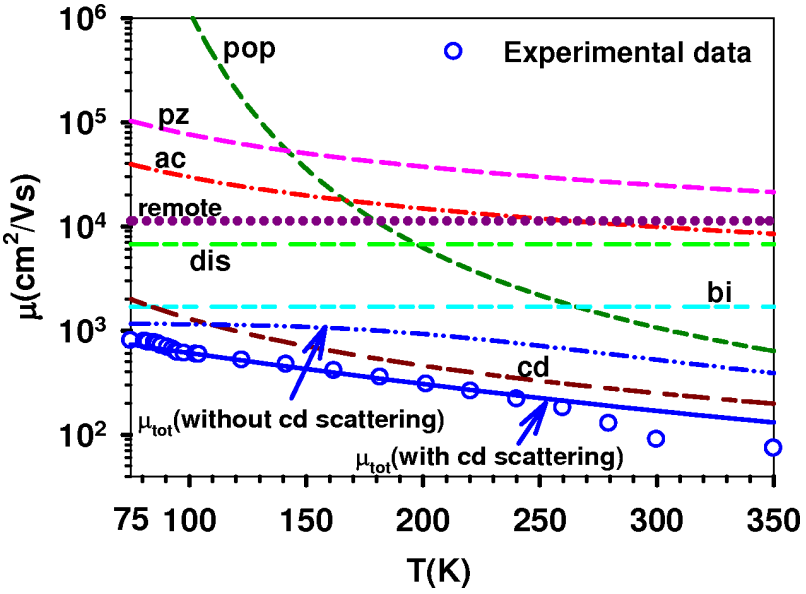

FIG. 2: 2DEG mobility versus temperature [7]. Each of the scattering mechanisms involved in controlling the mobility are observed.

TABLE IV: Fitting parameters of the 2DEG in the AlGaN/GaN system.

Dislocation density N_{disl} (cm^{-2})	1.3×10^{10}
2D impurity density in the potential well N_{bi} (cm^{-3})	1×10^{19}
Piezoelectric constant h_{14} (V/m)	4.5×10^9
C parameter	1.3×10^6

As seen in Fig. 2, the μ vs T experimental data, with consideration of the scattering mechanisms as mentioned in Section II, do not fit very well. In our analysis of the μ vs T experimental data, the extra scattering effect has been accounted for by an empirical mobility limit of the form of $C/T^{1.5}$ (crystal defect (cd) scattering mechanism) [18]. This empirical mobility limit has a dominant effect on the carrier mobility, especially in the high temperature region. Though the exact origin of the particular scattering mechanisms that keeps the high temperature mobility lower than expected are not known, they are very

TABLE V: Fitting parameters of the 2DEG in the AlGaN/GaN system with different electron effective masses.

Dislocation density N_{disl} (cm^{-2})	1.3×10^{10}
2D impurity density in the potential well N_{bi} (cm^{-3})	5.5×10^{18}
Piezoelectric constant h_{14} (V/m)	4.5×10^{9}
C parameter	2.2×10^{6}

likely to be related to the various kinds of crystalline defects, such as domain boundaries and strain induced fields (which are seen in the C parameter) that are known to exist at substrate levels in heteroepitaxial grown GaN material [17].

As seen in Fig. 2, at high temperature (260 to 350 K), the theoretical mobility is higher than the experimental motilities of the AlGaN/GaN heterostructure. In order to fit the high temperature mobility data, I have to change some material parameters of GaN. I can obtain a good fit for the high temperature by changing the value of the electron effective mass in this system. As seen in Fig. 3, with this change, the polar optical phonon has come lower compared to the previous level (Fig. 2). In this case, I have considered $m^* = 0.47m_0$ and the related fitting parameters can be seen in Table V. Though the exact origin of the changing of value of m^* still needs to be identified and discussed more.

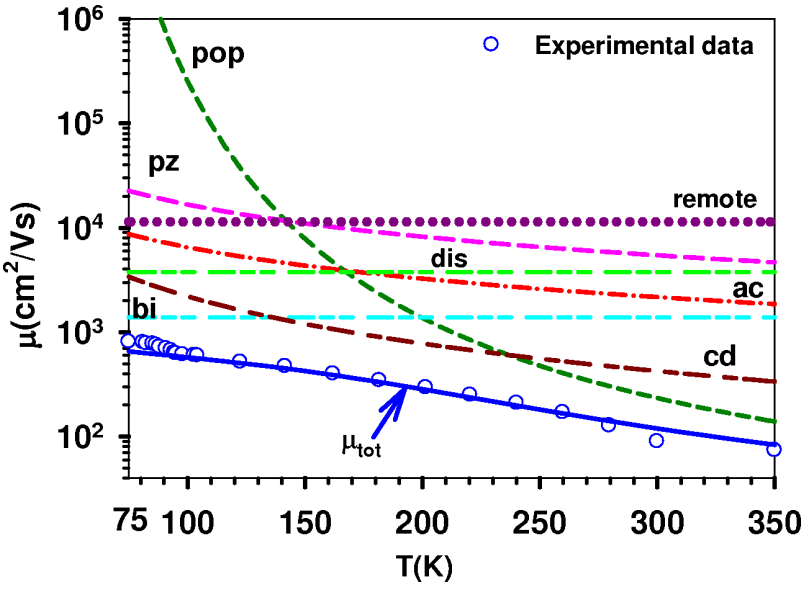

FIG. 3: 2DEG mobility versus temperature [7] by considering different electron effective masses.

The fitting parameters obtained in this table show:

An N_{disl} match with the accuracy of the reported values [19], in this matter in the range 10^9 to 10^{11} cm^{-2}. With consideration of the quantum well width of about 20 nm, N_{bi}

is comparable to the 2DEG bulk concentration value at the interface, that is consistent with our expectation. Finally, a magnitude of the piezoelectric constant (as a fitting parameter (it has not been reported for GaN yet)) comparable in magnitude and much greater than the value reported for GaAs ($= 2.1 \times 10^9$ V/m) [20] is obtained. The magnitude of the piezoelectric constant for this material can be considered as an acceptable value, especially with regard to its superior piezoeletric properties compared to GaAs. In addition, according to the results in Fig. 3 and the curve fitting drawn, the following points can be noted:

1 – In the medium temperature range ($75 < T < 230$ K), the ionized impurity due to the interface charge and crystal defect scattering mechanism is dominant.

2 – In the high temperature range ($230 < T < 350$ K) the polar optical phonon scattering mechanisms is dominant.

IV. CONCLUSION

In this paper, the electron transport properties of the 2DEG in an $Al_{0.3}Ga_{0.7}N/GaN$ heterostructure have been investigated, theoretically. Analysis of the μ vs T experimental data shows that the crystal defect, the ionized impurity due to the interface charges, and the polar optical phonon scattering mechanisms play important roles in controlling the carrier mobility in this system. Also, for obtaining a matched fit between the theoretical total mobility and experimental data in the high temperature range, the value of the electron effective mass (as a material parameter) should be changed to $0.47m_0$. Also, the piezoelectric constant, h_{14}, is obtained as 4.5×10^9 (V/m) as a fitting parameter.

Acknowledgement

I would like to thank H. Eshghi for technical assistance.

References

[1] B. Monemar, Phys. Rev. B **10**, 676 (1974). doi: 10.1103/PhysRevB.10.676
[2] S. Nakamura *et al.*, Jpn. J. Appl. Phys. Lett. **34**, L1332 (1995). doi: 10.1143/JJAP.34.L1332
[3] S. Nakamura *et al.*, Appl. Phys. Lett. **69**, 3034 (1996). doi: 10.1063/1.116830
[4] Z. Fan *et al.*, Electron. Lett. **33**, 814 (1997).
[5] M. A. Khan *et al.*, Appl. Phys. Lett. **66**, 1083 (1995). doi: 10.1063/1.113579
[6] Y. F. Wu *et al.*, IEEE Electron. Dev. Lett. **17**, 455 (1996).
[7] A. Y. Polyakov, L.-W. Jang, N. B. Smirnov, A. V. Govorkov, and E. A. Kozhukhova, J. Appl. Phys. **110**, 093709 (2011). doi: 10.1063/1.3658026
[8] K. Basu and B. R. Nag, Phys. Rev. B **22**, 4849 (1980). doi: 10.1103/PhysRevB.22.4849
[9] K. Lee, M. S. Shur, T. J. Drummond, and H. Morkoç, J. Appl. Phys. **54**, 6432 (1983). doi: 10.1063/1.331922
[10] P. J. Prince, Ann. Phys. NY **133**, 217 (1981).

[11] B. K. Ridley, J. Phys. C **15** 5899 (1982). doi: 10.1088/0022-3719/15/28/021
[12] K. Hess, Appl. Phys. Lett. **35**, 484 (1979). doi: 10.1063/1.91205
[13] H. Eshghi and M. Mootabian, Solid Sate Commun. **15**, 80 (2011).
[14] H. Morkoc and Umit Oagur, *Zinc Oxide Fundementals, Materials and Device Technology*, (Wiley-VCH, 2009).
[15] J. H. Davies, *The Physics of Low Dimensional Semiconductors*, (Cambridge University Press, 1998).
[16] H. Morkoc, *Handbook of Nitride Semiconductors and Devices*, (Wiley-VCH Verlag Gmbh, 2008).
[17] P. B. Perry, R. F. Rutz, Appl. Phys. Lett. **33**, 319 (1978). doi: 10.1063/1.90354
[18] H. Tang *et al.*, Solid State Electron. **42**, 839 (1998). doi: 10.1016/S0038-1101(98)00087-2
[19] D. Sugihara *et al.*, Jpn. J. Appl. Phys. **39**, L197 (2000). doi: 10.1143/JJAP.39.L197
[20] K. Lee, M. S. Shur, T. J. Drummond, and H. Morkoç, J. Appl. Phys. **54**, 6432 (1983). doi: 10.1063/1.331922